Available online at www.sciencedirect.com
ScienceDirect
Journal of Molecular Catalysis A: Chemical 266 (2007) 233–238
JOURNAL OF MOLECULAR CATALYSIS A: CHEMICAL
www.elsevier.com/locate/molcata

Responsive catalysis of thermoresponsive micelle-supported gold nanoparticles

Yao Wang [a], Guangwei Wei [a], Wangqing Zhang [a,*], Xiaowei Jiang [a], Peiwen Zheng [a], Linqi Shi [a], Anjie Dong [b]

[a] *Key Laboratory of Functional Polymer Materials, Institute of Polymer Chemistry, Nankai University, Tianjin 300071, China*
[b] *Department of Polymer Science and Technology, Tianjin University, Tianjin 300070, China*

Received 22 July 2006; received in revised form 30 October 2006; accepted 3 November 2006
Available online 11 November 2006

Abstract

The block copolymer poly(*N*-isopropylacrylamide)-*b*-poly(4-vinyl pyridine) (PNIPAM-*b*-P4VP) self-assembled into core-corona micelles with the P4VP block as core and the thermoresponsive PNIPAM block as corona in water. The diameter of the micelles was about 40 nm and the lower critical solution temperature (LCST) was about 32 °C. Gold nanoparticles of size ranging from 2 to 4 nm were loaded in the micelles to form a responsive catalyst, the activity of which could be modulated due to the thermoresponsive PNIPAM. Below LCST, the PNIPAM chains were hydrophilic and the reactants could easily diffuse through the PNIPAM corona to reach the surface of the gold nanoparticles. Within this temperature range, the catalytic activity of the micelle-supported gold nanoparticles increased with the increase in temperature. Above LCST, the PNIPAM chains collapsed to form a hydrophobic barrier on the gold nanoparticles, which decelerated diffusion of the reactants. Within this temperature range, the activity of the micelle-supported gold nanoparticles decreased with the increase in temperature until to a minimum constant at about 38 °C.

Keywords: Block copolymer; Gold nanoparticles; Micelles; Responsive catalyst; Thermoresponsive

1. Introduction

Highly selective and robust catalyst has been one of the most important topics in scientific literatures [1–5]. This strongly stimulates the development of new catalysts. Among such ones, polymer-supported catalysts where metal particles are located in polymeric matrix are expected to be promising [6]. To prepare highly dispersed polymer-supported catalysts, stabilizing agents such as functionalized polymers [7–11], dendrimers [12,13], and micelles [14–16] are usually used. Of all the polymers, poly(*N*-isopropylacrylamide) (PNIPAM) and their derivatives exhibit inverse temperature solubility and have a lower critical solution temperature (LCST) in water [17]. That is also to say, the PNIPAM chains are hydrophilic and soluble in water below LCST and become hydrophobic in water above LCST. The thermoresponsive polymers have been used to prepare responsive catalysts, the activity of which reversibly turns first off and then on as temperature is first raised and then lowered due to changes in the polymer-support's solubility [18–21]. Compared with common catalysts, the responsive catalyst has two advantages. Firstly, the catalysis can be easily modulated just by changing temperature. Secondly, the thermoresponsive catalyst can be easily recovered by heating the aqueous solution [18–20]. Facile synthesis of responsive catalysts is a challenge and interest to both industrial and academic chemists.

Up to present, micelles of coordination block copolymer such as polystyrene-*b*-poly(4-vinylpyridine) have been used to stabilize colloidal metal nanoparticles [22]. In such micelles, the nonpolar block forms the corona, which provides stabilization, while the polar block forms the core, which is able to dissolve metal compounds due to coordination [16]. Such micelles can be considered as nanoreactors or templates [23], where nucleation and growth of metal nanoparticles are restricted to the mesoscale level. Some colloids of monometallic catalysts and bimetal-

* Corresponding author at: Key Laboratory of Functional Polymer Materials, Institute of Polymer Chemistry, Nankai University, Tianjin 300071, China. Tel.: +86 22 23509794; fax: +86 22 23503510.
E-mail address: wqzhang@nankai.edu.cn (W. Zhang).

1381-1169/$ – see front matter © 2006 Elsevier B.V. All rights reserved.
doi:10.1016/j.molcata.2006.11.014

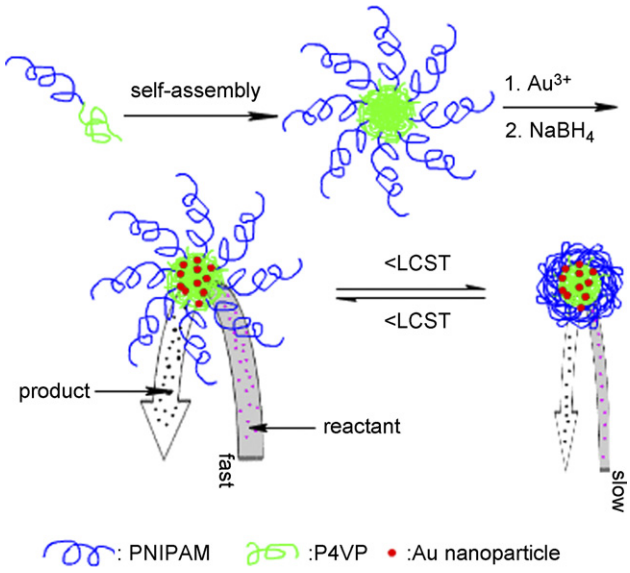

Scheme 1. Synthesis and responsive catalysis of the thermoresponsive micelle-supported gold nanoparticles, where the reduction of *p*-nitrophenol by $NaBH_4$ was chosen as a model reaction. The purple dots represent *p*-nitrophenol and the black dots *p*-aminophenol.

lic catalysts have already been synthesized by this method [22,23].

Herein, thermoresponsive micelle-supported gold nanoparticles and their responsive catalysis were studied. The thermoresponsive colloidal dispersion of micelle-supported gold nanoparticles was firstly prepared by loading gold nanoparticles in the thermoresponsive micelles of poly(*N*-isopropylacrylamide)-*b*-poly(4-vinyl pyridine) (PNIPAM-*b*-P4VP) due to coordination between $AuCl_4^-$ and the micelles [16]. Then, the thermoresponsive colloidal dispersion was used as responsive catalyst in reduction of *p*-nitrophenol with $NaBH_4$ to *p*-aminophenol. Below LCST, the PNIPAM chains in the polymer-supported catalyst were hydrophilic and the hydrophilic reactants such as *p*-nitrophenol and $NaBH_4$ could easily reach on the catalyst surface of the gold nanoparticles to arouse reaction. On the other hand above LCST, the PNIPAM chains collapsed on the gold nanoparticles surface to form a hydrophobic barrier to prevent or decelerate reaction. Scheme 1 shows the reaction catalyzed with the thermoresponsive micelle-supported gold nanoparticles.

2. Experimental

2.1. Materials

Methyl 2-chloropropanoate ($CH_3CHClCOOCH_3$ >96%) was purchased from Tokyo Kasei Kogyo Co. Ltd and used as received. The monomer 4-vinyl pyridine (4VP >95%) and the catalyst CuCl (>99%) were purchased from Aldrich and purified according to reference described elsewhere [24]. The monomer *N*-isopropylacrylamide (NIPAM, >99%, Acros Organics) was purified by recrystallization from a benzene/*n*-hexane mixture and dried carefully in a vacuum. Tris[2-(dimethylamino)ethyl]amine (Me_6TREN) was synthesized according to Ref. [24]. $HAuCl_4{\cdot}3H_2O$ (>99.9%), $NaBH_4$ (>98.9%) were purchased from Tianjin Chemical Company and used as received. Double-distilled water was used in this study. Other analytical reagents were used as received.

2.2. Synthesis of the block copolymer PNIPAM-b-P4VP by ATRP

The block copolymer $PNIPAM_{126}$-*b*-$P4VP_{34}$, where the subscripts represented the polymerization degree of the corresponding monomers, was synthesized by sequential atom transfer radical polymerization (ATRP) of *N*-isopropylacrylamide and 4-vinylpyridine.

The macroinitiator of chlorine-tailed poly(*N*-isopropylacrylamide) ($PNIPAM_{126}$-Cl) was firstly synthesized in toluene by ATRP using $CH_3CHClCOOCH_3$ as initiator and CuCl/Me_6TREN as catalyst. To a flask 0.12 g of $CH_3CHClCOOCH_3$, 0.46 g of Me_6TREN and 0.14 g of CuCl were added and then was added 12 mL of toluene. The mixture was first stirred and then degassed under nitrogen purge. Subsequently, 15.0 g of NIPAM was added into the flask and degassed under nitrogen purge again. Polymerization was performed at 40 °C for 4 h. The monomer conversion in 4 h was over 90%. The resultant polymer of $PNIPAM_{126}$-Cl was purified by first being dissolved in CH_2Cl_2 and then passed through an Al_2O_3 column to remove the copper catalyst and then deposited in a mixture of *n*-hexane and CH_2Cl_2 (8:2, v/v). The product was then dried under vacuum at 30 °C. The molecular weight M_W and polydispersity index PDI of $PNIPAM_{126}$-Cl measured by gel permeation chromatography (GPC) were 1.54×10^4 g/mol and 1.08, respectively. GPC measurement was performed on a Waters 600E gel permeation chromatography (GPC) analysis system, where DMF was used as eluent and narrow-polydispersity polystyrene was used as calibration standard. The GPC traces of the macroinitiator $PNIPAM_{126}$-Cl are shown in Fig. 1.

The block copolymer $PNIPAM_{126}$-*b*-$P4VP_{34}$ was synthesized by ATRP in 2-propanol using $PNIPAM_{126}$-Cl as macroinitiator and CuCl/Me_6TREN as catalyst. To a flask 0.12 g of Me_6TREN, 0.037 g of CuCl and 6 mL of 2-propanol was added and then was added 3.0 g of $PNIPAM_{126}$-Cl. The mixture

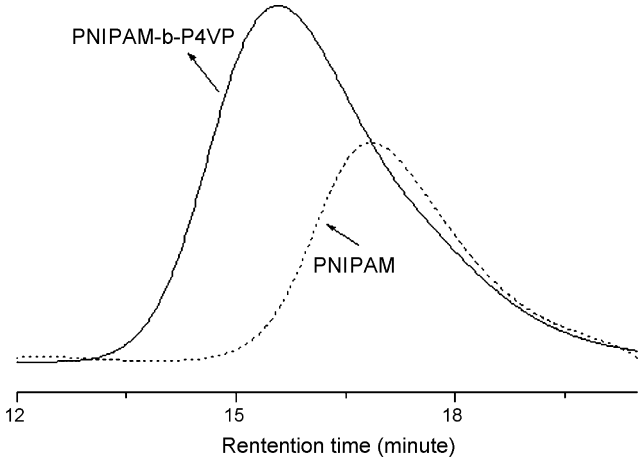

Fig. 1. The GPC traces of $PNIPAM_{126}$ and $PNIPAM_{126}$-*b*-$P4VP_{34}$.

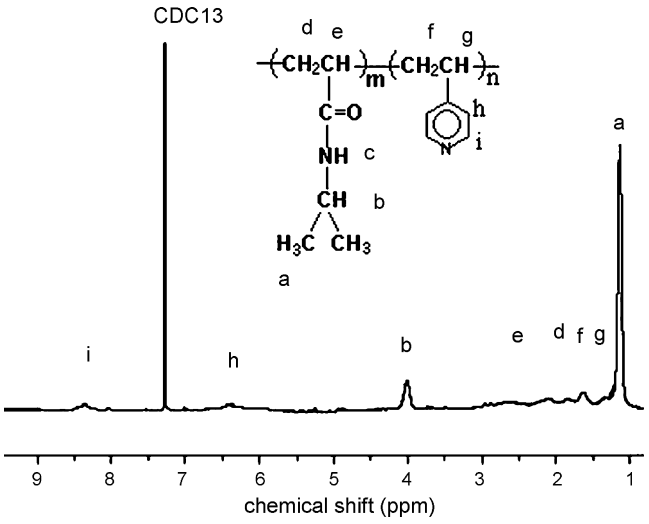

Fig. 2. The H NMR spectra of $PNIPAM_{126}$-*b*-$P4VP_{34}$ in $CDCl_3$.

was first stirred and then degassed under nitrogen purge. Subsequently, 1.2 g of 4-vinylpyridine was added into the flask and the mixture was degassed under nitrogen purge again. Polymerization was performed at 40 °C for 6 h. The monomer conversion was over 80%. The resultant block copolymer $PNIPAM_{126}$-*b*-$P4VP_{34}$ was purified by first being dissolved in CH_2Cl_2 and then passed through an Al_2O_3 column to remove the copper catalyst and then deposited in cold ether. The product was then dried under vacuum at 30 °C. The PDI of $PNIPAM_{126}$-*b*-$P4VP_{34}$ measured by GPC was 1.20 and the GPC traces are also shown in Fig. 1. The composition of the block copolymer $PNIPAM_{126}$-*b*-$P4VP_{34}$ was determined by ^1H NMR spectra as shown in Fig. 2, wherein the ^1H NMR spectra of the copolymers in $CDCl_3$ were recorded using a VARIAN UNITY PLUS-400 spectrometer.

2.3. Preparation of the micelles and micelle-supported gold nanoparticles

The core-corona micelles of $PNIPAM_{126}$-*b*-$P4VP_{34}$ were prepared by directly dispersing the block copolymer in water at pH 6.5 at room temperature, where the copolymer concentration was 0.50 mg/mL. The colloidal dispersion of micelle-supported gold nanoparticles was prepared as follows: 12.0 mL of 1.0 mmol/L $HAuCl_4$ aqueous solution at pH 6.5 was added into 40.0 mL of the micellar solution, where the molar ratio of the nitrogen atom in the P4VP block to $AuCl_4^-$ was about 6:1. The mixed solution was kept for about 1 h to allow for the coordination between $AuCl_4^-$ and the micelles and then 8.0 mL of 10.0 mmol/L $NaBH_4$ aqueous solution was added with vigorously stirring. The concentration of block copolymer and the gold nanoparticles in the colloidal dispersion was 0.33 mg/mL and 0.20 mmol/L, respectively.

2.4. Determination of cloud-point temperature

The cloud-point temperature or LCST of the $PNIPAM_{126}$-*b*-$P4VP_{34}$ micelles and the colloidal dispersion of micelle-supported gold nanoparticles were determined by measuring the absorbance or transmittance at 500 nm on a TU-8110 UV-vis spectrophotometer. The samples were heated by being directly immersed in preheated water at a given temperature and then the absorbance or transmittance was measured. The cloud-point temperature or LCST was defined as the temperature at the initial break point in the resulting transmittance versus the temperature curve.

2.5. Transmission electron microscopy (TEM) measurement

TEM measurement was conducted by using a Philips T20ST electron microscope at an acceleration voltage of 200 kV, whereby a small drop of the colloidal dispersion of micelle-supported gold nanocomposite was deposited onto a piece of copper EM grid, and dried at atmospheric pressure.

2.6. Catalytic reduction of p-nitrophenol

The catalytic reduction was conducted in a standard quartz cell with a path length of 1 cm. The initial molar ratio of Au/*p*-nitrophenol/$NaBH_4$ was 1/5/167. 1.0 mL of 10.0 mmol/L $NaBH_4$ aqueous solution was firstly mixed together with 1.5 mL of 0.20 mmol/L 4-nitrophenol aqueous solution (pH 6.5 adjusted by 1 mol/L NaOH aqueous solution) and then the mixture was heated to a given temperature. Immediately after addition of 0.30 mL of the preheated colloidal dispersion of micelle-supported gold nanoparticles with gold nanoparticle concentration at 0.20 mmol/L, the absorption spectra were recorded by a TU-8110 UV-vis spectrophotometer.

2.7. Recovery and reuse of the catalyst

The catalyst of colloidal dispersion of micelle-supported gold nanoparticles was recovered by firstly keeping the temperature at 4 °C and then dialyzing the colloidal dispersion against water at room temperature to remove all the reactants. The recovered catalyst was reused in another run with the molar ratio of Au/*p*-nitrophenol/$NaBH_4$ kept constant at 1/5/167.

3. Results and discussions

3.1. Synthesis and characterization of the micelle-supported gold nanoparticles

Since the PNIPAM block was hydrophilic and the P4VP block was hydrophobic at room temperature, the block copolymer of $PNIPAM_{126}$-*b*-$P4VP_{34}$ self-assembled into core-corona micelles in water with the P4VP block as core and the PNIPAM block as corona. When $AuCl_4^-$ was added into the micellar solution, it first coordinated with the P4VP block, and then was reduced to form micelle-supported gold nanoparticles. The typical TEM images of the micelle-supported gold nanoparticles are shown in Fig. 3. As shown in Fig. 3A and B, a large number of gold nanoparticles were formed in each micelle [25]. The average diameter of the micelles observed by TEM was about 40 nm. The gold nanoparticles loaded in the micelles ranged from 2 to 4 nm and the mean size was 3.3 nm (standard deviation,

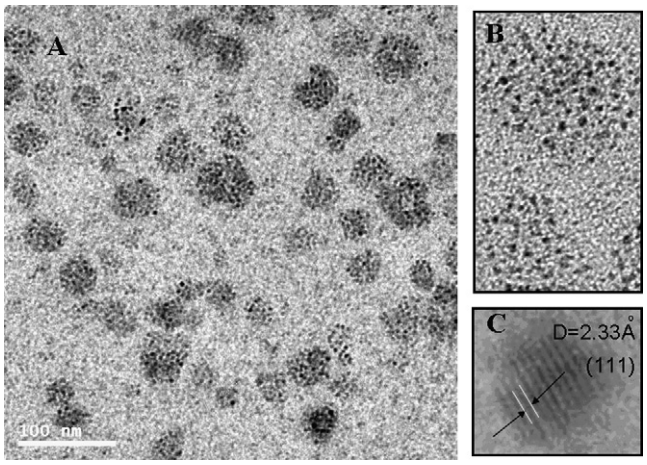

Fig. 3. TEM image of the micelle-supported gold nanoparticles (A), magnification of the TEM image of the micelle-supported gold nanoparticles (B), high-resolution TEM image of single gold nanoparticle in the micelle-supported gold nanoparticles (C).

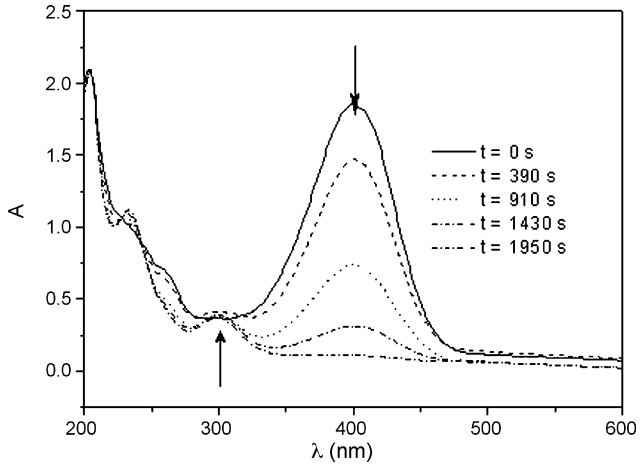

Fig. 5. Successive UV–vis absorption spectra of the reduction of 4-nitrophenol catalyzed with the thermoresponsive micelle-supported gold nanoparticles, where the concentration of 4-nitrophenol, $NaBH_4$ and gold was 0.107, 3.57 and 0.0214 mmol/L, respectively.

S.D. = 0.2 nm). Additionally, the multiple lattice fringes with an interplanar spacing of 2.33 Å (consistent with the interplanar distance of (1 1 1) plane) was observed clearly in the high-resolution TEM image as shown in Fig. 3C, which confirmed the formation of crystalline gold nanoparticles.

Fig. 4 shows the temperature dependence of light transmittance of the aqueous solutions of the thermoresponsive micelles and the colloidal dispersion of the micelle-supported gold nanoparticles. Both the micelles and the colloidal dispersion of micelle-supported gold nanoparticles showed a LCST or cloud-point temperature at about 32 °C. This suggested that the micelles and colloidal dispersion of micelle-supported gold nanoparticles could stably suspend in water below 32 °C; when temperature further increased to above 38 °C, the micelles and the micelle-supported gold colloidal dispersion became hydrophobic and the colloids became unstable. However, deposition only took place when temperature was above 50 °C. Furthermore, when the deposit was cooled in a refrigerator at about 4 °C, the deposit disappeared and the micelles or the micelle-supported gold colloidal dispersion recovered. This suggested that the micelle-supported gold nanoparticles could act as a recyclable catalyst.

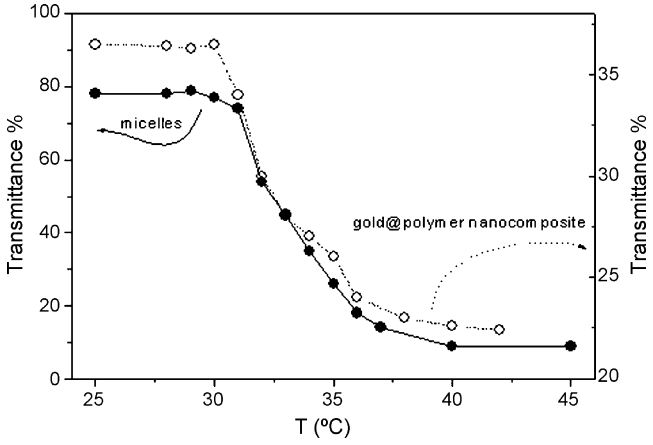

Fig. 4. Temperature dependence of light transmittance of the aqueous solutions of the core-corona micelles and the micelle-supported gold nanoparticles colloidal dispersion, where the block copolymer concentration was 0.33 mg/mL.

3.2. Reduction of p-nitrophenol catalyzed by micelle-supported gold nanoparticles

Herein, the reduction of *p*-nitrophenol by $NaBH_4$ was used as a model reaction to characterize the responsive catalysis of the thermoresponsive micelle-supported gold nanoparticles. To simplify the analyses, the concentration of $NaBH_4$ was set to exceed that of *p*-nitrophenol by far and the catalyst concentration of the micelle-supported gold nanoparticles kept a relatively low constant in all runs. Fig. 5 displays a typical example of such an analysis performed at 25 °C. Clearly, the characteristic peak of *p*-nitrophenol at 400 nm decreased with the increase in time, and a new peak at 290 nm appeared due to the formation of *p*-aminophenol [26,27]. Additional experiments demonstrated that no reduction took place without the micelle-supported gold nanoparticles. Therefore, it was evident that the conversion was due to the presence of the catalyst of the micelle-supported gold nanoparticles.

In the above-mentioned model reaction, the kinetics of the reduction can be treated as pseudo-first-order in *p*-nitrophenol concentration. The absorbance A_t at time t divided by the absorbance A_0 measured at $t = 0$ gives the corresponding concentration ratios C/C_0 of *p*-nitrophenol. Thus we get the following equation:

$$\frac{dC_t}{dt} = K_{app}t \quad \text{or} \quad \ln\frac{C_0}{C_t} = \ln\frac{A_0}{A_t} = K_{app}t \tag{1}$$

where C_t is the concentration of *p*-nitrophenol at time t and K_{app} is the apparent rate constant. Fig. 6A shows the linear plot of $\ln(C/C_0)$ versus t at different temperatures (some plots were not shown to simplify the figure). Based on the linear plots, the values of the apparent rate constant K_{app} at different temperatures were calculated, which are shown in Fig. 6B. Clearly,

Table 1
Reuse of the micelle-supported gold nanoparticles at temperature below and above LCST

Cycles	25 °C		40 °C	
	K_{app} ($\times 10^{-3}$ s^{-1})	TOF (h^{-1})	K_{app} ($\times 10^{-4}$ s^{-1})	TOF (h^{-1})
	1.48	15.5	5.93	12.0
First reuse	1.44	14.8	5.63	11.6
Second reuse	1.45	14.9	5.76	11.8
Third reuse	1.44	14.8	5.60	11.3

the value of K_{app} increased with the increase in temperature in the range from 25 to 30 °C. The possible reason was that the corona-forming PNIPAM chains were hydrophilic within this temperature range and the reactants could easily diffuse through the PNIPAM corona to reach the surface of the gold nanoparticles. Based on the Arrhenius equation, the rate usually increases with the increase in temperature. Sawant et al. also found the rate of hydrogenation of *p*-nitrophenol to *p*-aminophenol increases with the increase in temperature [28]. These suggest the present thermoresponsive micelle-supported gold nanoparticles are similar to those of general catalysts when the reduction is performed at temperature below LCST of the micelles. However, when temperature further increased to above LCST, the value of K_{app} decreased till to a constant with the increase in temperature at about 38 °C, which seemed abnormal compared with those general catalytic reduction [28]. The possible reason was that the PNIPAM chains collapsed to form a hydrophobic barrier on the gold nanoparticles at this temperature, which decelerated diffusion of the reactants onto the surface of the micelle-supported gold nanoparticles.

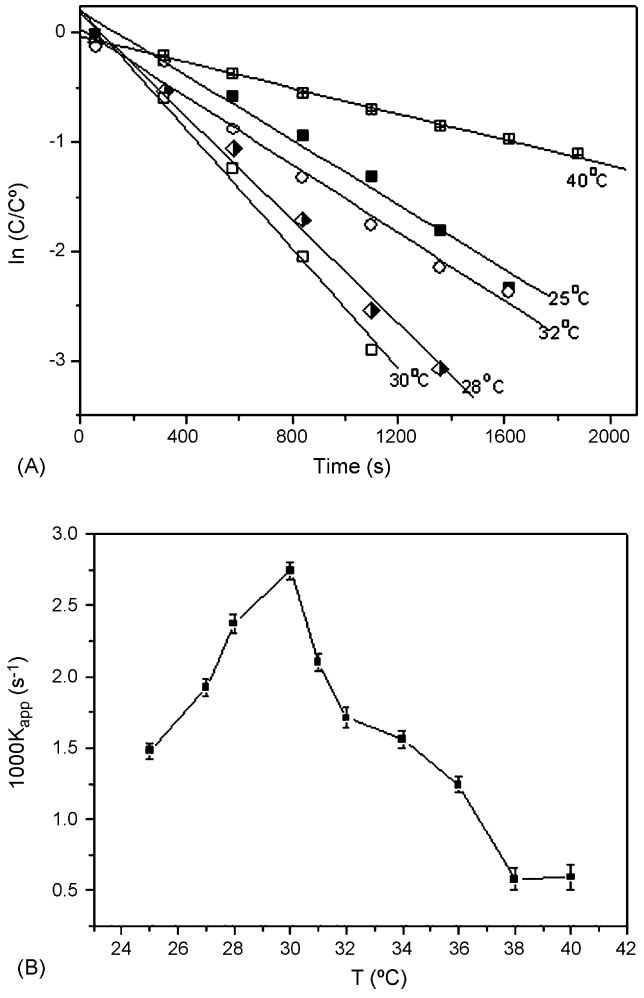

Fig. 6. Plots of concentration ratios C/C_0 of *p*-nitrophenol vs. times at different temperatures (A) and plots of the apparent rate constant K_{app} of the reduction catalyzed with the thermoresponsive micelle-supported gold nanoparticles (B). Reaction conditions as described in Fig. 5.

Based on the fitting line as shown in Fig. 6, the TOF value of the responsive catalyst with the conversion of *p*-nitrophenol at about 20% at 25 °C was estimated at 15.5 h^{-1}. Esumi et al., Pal et al. and Guibal et al. prepared the catalyst of gold-dendrimer nanocomposite, gold nanoparticles immobilized with anion exchange resin, chitosan-supported palladium nanoparticles and silver nanoparticles, respectively, and studied the catalytic reduction of *p*-nitrophenol [29–32]. The TOF values of the corresponding catalysts were not pointed out. Based on our approximate calculation, the TOF values were about 20, 16, 18 and 18 h^{-1}, respectively. This suggested that the present responsive catalyst was as efficient as those general catalysts at room temperature. The micelle-supported gold nanoparticles also showed excellent recyclability for the reduction at temperature below or above LCST (Table 1). The catalyst could be reused at least three times with no indication of the catalyst deactivation, which confirmed the high stability of these catalysts. The responsive catalyst had two characteristics. Firstly, its activity was responsive to temperature due to the thermoresponsive PNIPAM chains. Secondly, when the thermoresponsive micelle-supported gold-nanoparticle dispersion was kept cool at 4 °C, the catalyst could be recovered and the recovered catalyst was almost as efficient as the original one.

Conclusively, we have proposed a method for synthesis of a responsive gold catalyst of thermoresponsive micelle-supported gold nanoparticles. The micelle-supported gold nanoparticles act as a recyclable responsive catalyst, the catalytic activity of which accelerated first and then decelerated when temperature increased in the range below and above the LCST of the thermoresponsive nanocomposite. We anticipate that the proposed method can be used to prepare various responsive catalysts such as thermoresponsive micelle-supported Pd nanoparticles, Pt nanoparticles, Ag nanoparticles and so on.

Acknowledgements

The financial support by National Science Foundation of China (No. 20504016) and the Outstanding Scholar Program

of Nankai University is acknowledged. The authors also thank Dr. Xinlin Yang in Nankai University for his kind discussion.

References

[1] L.N. Lewis, Chem. Rev. 93 (1993) 2693.
[2] J.D. Aiken, R.G. Finke, J. Mol. Catal. A 145 (1999) 1.
[3] F. Porta, L. Prati, J. Catal. 224 (2004) 397.
[4] G. Mele, D.R. Sole, G. Vasapollo, E. Garcia-Lopez, L. Palmisano, M. Schiavello, J. Catal. 217 (2003) 334.
[5] G.M. Veith, A.R. Lupini, S.J. Pennycook, G.W. Ownby, N. Dudney, J. Catal. 231 (2005) 151.
[6] D.E. Bergbreiter, Catal. Today 42 (1998) 389.
[7] A. Tuchinsky, U. Zehavi, React Funct. Polym. 39 (1999) 147.
[8] R. Annunziata, M. Benaglia, M. Cinquini, F. Cozzi, Chem. Eur. J. 6 (2000) 133.
[9] R. Akiyama, S. Kobayashi, J. Am. Chem. Soc. 125 (2003) 3413.
[10] A.E. Kaifer, L. Strimbu, J. Liu, Langmuir 19 (2003) 483.
[11] J. Shan, M. Nuopponen, H. Jiang, E. Kauppinen, H. Tenhu, Macromolecules 36 (2003) 4526.
[12] K. Esumi, H. Houdatsu, T. Yoshimura, Langmuir 20 (2004) 2536.
[13] G.E. Oosterom, J.N.H. Reek, P.C.J. Kamer, P.N.M. van Leeuwen, Angew. Chem. Int. Ed. 40 (2001) 1828.
[14] S. Klingelho1fer, W. Heitz, A. Greiner, S. Oestreich, S. Forster, M. Antonietti, J. Am. Chem. Soc. 119 (1997) 10116.
[15] B.R. Cuenya, S.-H. Baeck, T.F. Jaramillo, E.W. McFarland, J. Am. Chem. Soc. 125 (2003) 12928.
[16] M.V. Seregina, L.M. Bronstein, O.A. Platonova, D.M. Chernyshov, P.M. Valetsky, J. Hartmann, E. Wenz, M. Antonietti, Chem. Mater. 9 (1997) 923.
[17] S. Fujishige, K. Kubota, I. Ando, J. Phys. Chem. 93 (1989) 3311.
[18] D.E. Bergbreiter, B.L. Case, Y.-S. Liu, J.W. Caraway, Macromolecules 31 (1998) 6053.
[19] C.-W. Chen, K. Arai, K. Yamamoto, T. Serizawa, M. Akashi, Macromol. Chem. Phys. 201 (2001) 2811.
[20] H. Hamamoto, Y. Suzuki, Y.M.A. Yamada, H. Tabata, H. Takahashi, S. Ikegami, Angew. Chem. Int. Ed. 44 (2005) 4536.
[21] Y. Lu, Y. Mei, M. Drechsler, M. Ballauff, Angew. Chem. Int. Ed. 45 (2006) 813.
[22] S. Forster, M. Antonietti, Adv. Mater. 10 (1998) 195.
[23] Y. Lou, M.M. Maye, L. Han, J. Luo, C.-J. Zhong, Chem. Commun. 5 (2001) 473.
[24] J. Xia, X. Zhang, K. Matyjaszewski, Macromolecules 32 (1999) 3531.
[25] M. Antonietti, E. Wenz, L. Bronstein, M. Seregina, Adv. Mater. 7 (1995) 1000.
[26] J. Liu, G. Qin, P. Raveendran, Y. Ikushima, Chem. Eur. J. 12 (2006) 2131.
[27] Y. Mei, G. Sharma, Y. Lu, M. Ballauff, M. Drechsler, T. Irrgang, R. Kempe, Langmuir 21 (2005) 12229.
[28] S.P. Bawane, S.B. Sawant, Appl. Catal. A 293 (2005) 162.
[29] K. Hayakawa, T. Yoshimura, K. Esumi, Langmuir 19 (2003) 5517.
[30] S. Praharaj, S. Nath, S.K. Ghosh, S. Kundu, T. Pal, Langmuir 20 (2004) 9889.
[31] T. Vincent, E. Guibal, Langmuir 19 (2003) 8475.
[32] N. Pradhan, A. Pal, T. Pal, Colloids Surf. A 196 (2002) 247.